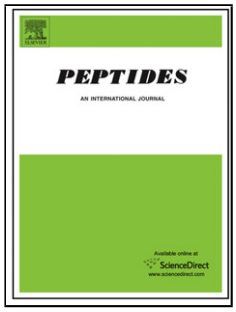

Title: Differential effects of hypo- and hyperthyroidism on remodeling of contacts between neurons expressing the Neuropeptide EI and Tyrosine Hydroxylase in hypothalamic areas of the male rat

Authors: Carolina Ayala, Gisela E. Pennacchio, Marta Soaje, Jackson C. Bittencourt, María E. Celis, Graciela Jahn, Susana R. Valdez, Alicia M. Seltzer

PII: S0196-9781(18)30258-4
DOI: https://doi.org/10.1016/j.peptides.2018.12.008
Reference: PEP 70054

To appear in: *Peptides*

Received date: 30 August 2018
Revised date: 10 December 2018
Accepted date: 22 December 2018

Please cite this article as: Ayala C, Pennacchio GE, Soaje M, Bittencourt JC, Celis ME, Jahn G, Valdez SR, Seltzer AM, Differential effects of hypo- and hyperthyroidism on remodeling of contacts between neurons expressing the Neuropeptide EI and Tyrosine Hydroxylase in hypothalamic areas of the male rat, *Peptides* (2018), https://doi.org/10.1016/j.peptides.2018.12.008

Differential effects of hypo- and hyperthyroidism on remodeling of contacts between neurons expressing the Neuropeptide EI and Tyrosine Hydroxylase in hypothalamic areas of the male rat

***Short running title**: Hypothalamic neurons and thyroid hormones*

Carolina Ayala[1,5], Gisela E. Pennacchio[2,3], Marta Soaje[2,6], Jackson C. Bittencourt[4], María E. Celis[5] , Graciela Jahn[2], Susana R. Valdez[2,3] and Alicia M. Seltzer[1]

1 Laboratorio de Neurobiología, Instituto de Embriología e Histología (IHEM-CONICET), Facultad de Ciencias Médicas, Universidad Nacional de Cuyo (UNCuyo), 5500, Mendoza, Argentina.

2 Laboratorio de Reproducción y Lactancia, Instituto de Medicina y Biología Experimental de Cuyo (IMBECU-CONICET), Centro Científico Tecnológico (CCT), 5500, Mendoza, Argentina.

3 Facultad de Ciencias Exactas y Naturales, UNCuyo, 5500, Mendoza, Argentina.

4 Department of Anatomy, Institute of Biomedical Sciences, University of Sao Paulo, Brazil.

5 Laboratorio de Ciencias Fisiológicas, Cátedra de Bacteriología y Virología Médicas, Facultad de Ciencias Médicas, Universidad Nacional de Córdoba., 5000 Córdoba, Argentina.

6 Instituto de Fisiología, Facultad de Ciencias Médicas, UNCuyo, 5500, Mendoza, Argentina.

Corresponding author:
Dr. Susana Ruth Valdez, IMBECU-CONICET.
Facultad de Ciencias Exactas y Naturales. Universidad Nacional de Cuyo. 5500 Ciudad de Mendoza MENDOZA-ARGENTINA Phone: 54-261-5244156
Email: svaldez@mendoza-conicet.gov.ar

Highlights

- •In the IHy we observed a remodeling of TH and NEI neuronal contacts in hypo- and hyperthyroid animals.
- •In the DL-PLH the thyroid hormones affect the dendritic trees without perturbing the NEI-TH contacts.
- •In the PLH NEI mRNA increased by hypothyroidism and TRH-R1 co-localized in the same neurons.
- •The hypothyroid status increased the interaction between the NEI neurons and the dopaminergic pathways.

Abstract

The Neuropeptide EI (NEI, glutamic acid- isoleucine amide) participates in neuroendocrine function. Previously we demonstrated that NEI concentration is regulated by thyroid hormones in discrete hypothalamic areas in rats. We observed that the thyroid status affects the dopaminergic regulation of the pituitary hormones. In this study we explored possible interactions between NEI and tyrosine hydroxylase (TH) containing elements in selected hypothalamic areas of male rats. Neuronal somas, terminals and boutons were assessed by confocal microscopy, in hypo- and hyperthyroid animals. We observed a remodeling of the contacts between the TH and NEI immunoreactive elements in the incerto-hypothalamic area (IHy, also known as rostromedial zona incerta) according to thyroid function. However, in the dorsolateral zone of the peduncular part of the lateral hypothalamus (DL-PLH) the thyroid hormones affect the dendritic trees of the neurons without perturbing the overall NEI/TH contacts. Also, we demonstrated that TRH Receptor 1 (TRH-R1) is colocalized in NEI immunoreactive neurons in the peduncular part of the lateral hypothalamus (PLH) and NEI precursor mRNA expression increased by hypothyroidism indicating that NEI neurons are responsive to the feedback mechanisms of the Hypothalamic Pituitary-Thyroid Axis (HPT). In conclusion, the hypothyroid status seems to increase the interactions between the NEI neurons and the dopaminergic pathways while the hyperthyroidism either decreases or display no effects. Altogether these observations support the participation of the IHy and PLH NEI as a modulating component of the HPT suggesting that altered neuroendocrine, behavioral and cognitive dysfunctions induced by dysthyroidism could be in part mediated by NEI.

Keywords: ***Neuropeptide (N) glutamic acid (E) isoleucine (I) amide (NEI), tyrosine hydroxylase (TH), hypothyroid status, hyperthyroid status, hypothalamus, Rostral/caudal incerto-hypothalamic area (IHy), Peduncular part of the lateral hypothalamus (PLH).***

Introduction

Neuropeptide glutamic acid isoleucine amide (NEI), melanin-concentrating hormone (MCH) and neuropeptide glycine-glutamic acid (NEG) derived from a common precursor, prepro-MCH (pp-MCH), function as neurotransmitters or modulators originating primarily from incerto-hypothalamic (IHy) and lateral hypothalamic (LH) areas [1, 2]. The NEI terminals of this system are thought to have a role on several physiological functions such as sensorimotor integration and the regulation of neuroendocrine functions related to motivated behaviors [3, 4]. NEI participates in neuroendocrine function and regulation of the reproductive axis [5, 6, 7] and in behavior, modulating grooming and locomotor activity [8, 9, 10, 11]. The regulatory action of NEI over endocrine, behavioral and autonomic processes can be explained by diverse and complex mechanisms. Anatomical and behavioral data suggest that physical interactions between NEI terminals and those of the dopaminergic system may occur in the ventral medial nucleus (VMN) of the hypothalamus. [12]. An early work by Kizer et al, [13] mentions a relationship between the catecholamines NA and DA (assessed by measuring TH activity) and thyroid hormones in the median eminence terminals. Also, a reduction in tyrosine hydroxylase messenger RNA levels was found in the arcuate nucleus of mutant mice devoid of all known thyroid hormone receptors [14].

There are two types of G protein-coupled receptors for TRH (Thyrotropin-releasing hormone) in rodents, subtype 1 (TRH-R1) and subtype 2 (TRH-R2). TRH-R1 mRNA is expressed in restricted regions of the hypothalamus including the lateral hypothalamus and the posterior hypothalamic area to control neuroendocrine and autonomous functions and the regulation of the HPT axis [15]. Our previous works reported that hypothyroidism and hyperthyroidism affects NEI content in selected brain areas of male and female rats [16,17].

In the present work we explored the possible interaction between dopamine/NEI neurons of adult male rats under three different hormonal conditions: eu-, hypo- and hyperthyroidism, in the rostral part of the rostromedial zona incerta (rostral-IHy), a location shared by NEI neurons and the dopaminergic A13 group [4]. We also examined the caudal part of the IHy (caudal-IHy) and a region located dorsal to the peduncular part of the lateral hypothalamus and lateral to the subincertal nucleus (according to the Atlas of Paxinos & Watson) [18] that we denominated DL-PLH (area that would correspond to the lateral hypothalamic nucleus, LHAm, described by Swanson et al.) [19,20]. The same experimental conditions and treatments were applied to study the interaction between NEI/TH and NEI/TRH-R1

immunoreactive neurons and nerve terminals and the NEI precursor (pp-MCH), TH and TRH-R1 mRNA expression in the peduncular part of the lateral hypothalamus (PLH).

Materials and Methods

Experimental Animals

Adult male Wistar rats aged 11 – 13 weeks and weighing 250 – 320 g, bred in the Instituto de Medicina y Biología Experimental de Cuyo (IMBECU)-CONICET, were maintained on a 14/10-h light/dark cycle in a temperature-controlled environment (22 ± 2°C) with *ad-libitum* access to standard rat chow and water. The procedures performed in animals were consistent with the standards established by the National Institutes of Health Guide for the Care and Use of Laboratory Animals (2011) and the American Veterinarian Medical Association Guidelines on Euthanasia. A total of 48 animals were divided into control and treated. Control (euthyroid): maintained in the same conditions of temperature and humidity as the treated ones (n=16); hypoT (hypothyroidism): received 6-propyl-2-thiouracil (PTU, Sigma) at a concentration of 0.1 g/l administered in the drinking water for 21 days (n=16); hyperT (hyperthyroidism): received L-thyroxine (L-T_4, Sigma) 250 µg/kg administered subcutaneously for 21 days (n=16). We have previously shown that these treatment regimens induce changes in T_3, T_4 and TSH consistent with hypo and hyperthyroid states [16,17].

Tissue preparation for immunohistochemistry

Six animals from each group were deeply anesthetized with chloral-hydrate 30% and perfused through the left cardiac ventricle with 150 ml of washing solution (0.8% w/v NaCl, 0.8% w/v sucrose, 0.4% w/v glucose and 0.35 M Na_2SO_3) and then with 200 ml of 4% paraformaldehyde (Sigma-Aldrich) in 0.01 M phosphate buffer (PBS) pH: 7.4 + 0.35 M Na_2SO_3. Brains were cryo- protected with increasing concentrations of sucrose (10, 20 and 30 % w/v in PBS 0.01 M pH 7.4), washed and stored at minus 70°C; 30-µm thick coronal sections were cut throughout the rostral forebrain region (from 0.12 mm to –3.48 mm from Bregma) using a cryostat (MICROM HM 505E) and stored at 4 – 8 °C in PBS + 0.03 % NaN_3.

Selection of the areas of interest

The areas of interest were selected following a series of criteria: physiological regarding the known or estimated function of the area and anatomical considering previous known presence of NEI and TH cells and fibers [2, 3, 4, 6, 21, 22]. First, we corroborated by DAB (3,3' Diaminobenzidine) immunostaining that the entire distribution of NEI cells and quantity was the same under the three conditions (eu-, hypo-and hyperthyroidism). Images were taken at 4x, 10x and 40x in an optical microscope and and quantified at largest magnification.

Double-labeling fluorescence immunohistochemistry to identify NEI, TH and TRH–R1 neurons and fibers

The coronal slices (30μm) from each brain were selected according to the areas of interest following the parameters of the Atlas of Paxinos 7th Edition [18]. We used slices obtained at approximately –2.16 mm from Bregma containing the rostral part of the incerto-hypothalamic area (rostral-IHy), (Fig. 1A) and at -2.76 mm from Bregma including a caudal part of the incerto-hypothalamic area (caudal-IHy), a region located dorsal to the peduncular part of the lateral hypothalamus and lateral to the subincertal nucleus (DL-PLH) and also the peduncular part of the lateral hypothalamus (PLH) (Fig. 1A-C). Sections of control, hypoT and hyperT groups were immunostained for NEI and TH, or TRH-R1 and NEI, using free-floating immunohistochemistry. In the first case, tissues were washed with PBS 0.01 M and treated for antigen retrieval with 0.01 M sodium citrate buffer pH: 6.0 at 95 °C for 5 minutes, washed again and then incubated in blocking solution (PBS 0.01 M with 0.3% Triton X-100 and 1% goat serum) for 1 hour followed by incubation with primary antibody rabbit polyclonal anti-NEI, Code PBL#237 antiserum [2], kindly provided by Sawchenko PE and Bittencourt JC, (The Salk Institute, La Jolla, CA). The antibody dilution used was 1:1000 (diluted in incubation solution PBS containing 0.3% Triton X-100 + 1% goat serum) for 24 h at 4 °C. After washes in PBS, tissues were incubated with the secondary antibody, sheep anti-rabbit FITC (IgG, F-7512, Sigma-Aldrich) dilution 1:250 in PBS + 1% goat serum for 90 min. After three consecutive PBS washes, sections were incubated in blocking solution (PBS 0.01 M with 0.1% Triton X-100 and 5% goat serum) for 1 hour and dopaminergic somas and terminals were labeled with the corresponding primary antibody mouse anti-TH for 24 h at 4 °C (anti TH, Code TOH A1.1[23] diluted 1:150, generously provided by Dr. C. Cuello,

McGill University) and then incubated with anti-mouse Cy5 (Jackson Immunoresearch, dilution 1:200) in PBS 0.01 M + 0.5% goat serum,) for 90 min. In the second case, TRH-R1 and NEI, after antigen retrieval with citrate buffer, tissues were washed and incubated in blocking solution (PBS 0.01 M with 0.2% Triton X-100 and 1% horse serum) for 1 hour followed by incubation with primary antibody goat anti-TRH-R1 (I-20) Cod. Sc-11574 Santa Cruz Biotecnology Inc., diluted 1:100 during 24 h at 4 °C, washed and incubated with the secondary antibody anti-goat Alexa 568 (A11057, Invitrogen), dilution 1:200 in PBS 0.01 M + 0.5% goat serum, for 90 min. After, tissues were washed and blocked with PBS containing 0.3% Triton X-100 + 1% goat serum to follow the incubation with NEI as was explained before. Finally, sections were washed and mounted in gelatin-chromium (III) potassium sulfate coated slices and incubated with ProLong® Gold DAPI (Invitrogen, P36935) and protected from light at 4 °C until analysis. When primary or secondary antibodies were routinely omitted resulted in the complete absence of immunofluorescence signal.

Image acquisition and processing

To assess remodeling in selected somas, terminals and boutons we applied previously validated tools of confocal microscopy [24, 25]. Tissue was examined using a confocal microscope (Olympus FV-1000). Only isolated neurons, non-overlapped with other positive stained elements, were selected with a 20x objective and acquired with 60x oil lens in multichannel mode [Fig. 1]. All images were acquired at -2.16 and at -2.76 mm; NEI and TH somas were observed mostly at -2.16 mm from Bregma [Fig. 2A and 5A] while terminals predominated at -2.76 mm from Bregma [Fig. 1G, H, J, K; Fig. 2D and G; Fig. 6B and C]. In addition, at -2.76 mm from Bregma images were acquired to assess NEI somas and TRH-R1 immunolabeled elements [Fig. 6 D-I]. Solid-state lasers were used to excite the FITC and Cy5 fluorochromes at 519 and 664 nm and the Alexa-568 fluorochrome at 572 nm, respectively. All images from the different experimental groups were digitized with identical microscope settings and image size and stored as .oib files. In this case, omission of primary or secondary antibodies resulted in an almost complete negative (i.e., dark) image (results not shown). NEI/TH immunofluorescence images were obtained by lineal and sequential mode, xyz (z=1.3 μm/plane), pinhole 110 μm and Kalman 3, 640 x 640 pixels. First, .oib images were converted to .oif and the number of planes in the z stack was randomized to 15, each z plane of each stack was deconvoluted using parallel spectral deconvolution and the appropriate point spread function (PSF) using MacBiophotonics Image J 1.43 software. To

analyze the characteristics of NEI neurons and their relationship with dopaminergic components and the changes induced by hypo- and hyperthyroidism, each image was subdivided in standardized areas of 154 x 207 pixels containing a NEI neuron with the surrounding dopaminergic elements. The number of NEI cells considered in this analysis from all animals included in this study: control, hypoT and hyperT were 12, 21 and 8 in the rostral-IHy respectively; 26, 27 and 21 in the caudal-IHy and 27, 25 and 25 in the DL-PLH. To determine the intensity of labeling and the effect of treatments, NEI and TH immunoreactivity (IR) were analyzed in terms of optical density (OD) by Image J 1.45 software, for this purpose all planes of the z stack of each standardized area were grouped. Green and red channels were separated and converted to 8 bits and brightness and contrast were normalized. Results were expressed relative to the control group.

3D Analysis

To determine the effects of hypo- and hyperthyroidism on NEI and TH neurons, dendrites and boutons, a 3D analysis was made in the same regions and cell groups described above. In all regions and groups studied the total NEI and TH positive objects were counted using the "3D object counter" function, establishing the corresponding threshold and a minimum size filter of 10, the results obtained belong to the summatory of all elements. The relationship between NEI and DA neurons and terminals in the regions under study was determined using the "colocalization highlighter" function (Both functions are available in Image J 1.45 and FIJI-Image J software). Using Image J 1.45 a 3D reconstruction was made in the rostral-IHy of control, hypoT and hyperT sections and by rotating these 3D images it was possible to count the contacts between NEI and TH elements. In the case of NEI/TRH-R1 images were taken in the xy plane, processed by deconvolution and the image J 1.43 was used to apply Manders and Pearson coefficients to determined colocalization.

Real time PCR

Animals were sacrificed by swift decapitation; brains were removed and immediately placed in an aluminum plate at 4 °C for carrying out specific coronal rat brain slices (stainless steel brain slicer, model RBM 4000C, ASI, Intruments, Inc.). Bilateral PLH microdissection was done as was described previously in Ayala C. *et al* 2011 [16] and pooled for total RNA extraction. PLH samples were homogenized in 0.3 ml of TRIzol (GIBCO-BRL) and total RNA isolated according to the manufacturer's instructions. Total RNA concentrations were determined by spectrophotometry, and integrity of the RNA was examined by 1% agarose gel electrophoresis. First strand cDNA synthesis

from 2.5 µg RNA per sample was performed using Moloney murine leukemia virus retrotranscriptase and random hexamer primers (Invitrogen/Life Technologies, Buenos Aires, Argentina) in a 20 µl reaction mixture. Real-time quantification was monitored by measuring the increase in fluorescence caused by the binding of EvaGreen dye (Biotium) to double-strand DNA at the end of each amplification cycle. The cDNAs were amplified with rat-specific primers for precursor NEI (pp-MCH), TH and TRH-R1 and S16 in the conditions described in Supplementary Table 1. Samples were run in duplicate. Simultaneously, each PCR run included a no-template control and a sample without reverse transcriptase. Real-time PCR was performed with a Corbett Rotor Gene 6000 Real-Time Thermocycler (Corbett Research Pty Ltd (Sydney, Australia) in a final volume of 20 µl. The reaction mixture consisted of 2 µl of 10xPCR Buffer, 1 µl of 50 mM $MgCl_2$, 0.4 µl of 10 mM dNTP Mix (Invitrogen), 1 µl of 20 × Eva Green (Biotium), 0.25 µl of 5 U/µl Taq DNA Polymerase (Invitrogen), 0.1 µl of each 2.5 mM primer (forward and reverse primers) and 10 µl of diluted cDNA (See Table 1 in supplementary file for primer sequences). The PCR reactions were initiated with 5 min incubation at 95 °C, followed by 40 cycles of 95 °C for 30s, 60 °C for 30s and 72 °C for 30s (Supplementary Table 1). Relative levels of mRNA were normalized to S16 reference gene as established in previous work [26]. Cycle threshold (CT) versus input concentration was plotted and efficiencies for each primer pair calculated using the equation $E = 10^{-1/s} - 1$ where s is the slope. Melt curve analysis (60 °C–95 °C in 0.2 °C increments) was performed at the end of the amplification and some samples were subjected to 1.5% agarose gel electrophoresis to examine product purity and verify correct size for the PCR product. Relative expression was calculated using the $2^{-\Delta\Delta CT}$ method [27].

Statistical analysis

Data were analyzed using GraphPad Prism version 5.00 for Windows (GraphPad Software, San Diego California USA, www.graphpad.com). Statistical differences were determined by ANOVA-1 followed by Bonferroni multiple comparisons post-test. Results are expressed as mean ± SEM, a value of $p < 0.05$ was considered statistically significant.

Results

Effects of hypo- and hyperthyroidism in the IHy

NEI and TH (the dopamine synthesis rate limiting enzyme) immunoreactive elements (NEI-IR and TH-IR) were present in the IHy of the three groups of animals studied (control n=3, hypoT n=3 and hyperT n=3). In this area, the TH-IR mostly labels the dopaminergic A13 neurons. Dense networks of somas, fibers and terminals NEI-IR were identified in the rostral- and caudal- IHy. We observed both TH-IR somas and axons present in the rostral-IHy whereas only scarce TH-IR axons were found at caudal-IHy (Fig. 2A and D). In the hypoT animals NEI-IR increased significantly (rostral: $p<0.01$ vs control; caudal: $p<0.001$ vs. control and hyperT) in neurons and terminals present in this region (Figs. 2B and E), while in the hyperT animals NEI-IR increased significantly only the rostral-IHy ($p<0.05$). On the contrary, TH-IR fibers and somas in the rostral IHy, were not affected by treatments. In the caudal-IHy, hypoT significantly decreased TH-IR ($p<0.001$ vs. control and hyperT) (Figs. 2C and F). TH-IR axon varicosities, as expected, were found intermingled or in juxtaposition to the vast majority of NEI-IR neurons but not co-localized (Fig. 2A and D merge). The following step was to explore if the tissue architecture is modified by the hormonal milieu. We then performed a 3D analysis of individual NEI neurons and their surrounding elements. In the first place we observed that the number of objects associated with these neurons was modified by the treatments. Neurons from hypoT animals encompassed an increased and those from hyperT animals a decreased number of NEI-IR objects per NEI-IR cell in both the rostral and caudal regions of the IHy (Fig. 3A and B). On the other hand, TH-IR objects presented a different pattern: the somas, fibers and boutons were counted, considering them as a summatory of elements in the proximity, and they resulted significantly increased ($p<0.05$ vs control) in the rostral-IHy of hypoT animals, while hyperT was not significantly different from controls (Fig. 4A). On the contrary, the percentage of TH-IR elements in the caudal-IHy showed a different pattern, with marked decreases in the hypoT and hyperT rats ($p<0.001$ vs control) (Fig. 4B). Furthermore, values from hypoT rats were also significantly lower than the values from hyperT animals ($p<0.05$) (Fig. 4B). The results depicted above suggest a change in the architecture of the IHy area that depends on thyroid function. To prove this hypothesis we used the 3D reconstruction of the stacks, confirming the lack of overlapping of the signals from both neuronal groups (Fig. 5A-J). The results of the quantitative analysis showed that the number of total NEI-TH neuronal contacts increases significantly in both the rostral and caudal-IHy of the hypoT animals, and a differential response is observed under the hyperT status, showing no changes in the number of contacts in relation to the

control untreated (euthyroid) rats (Fig. 5K and L). These results suggest that in the IHy the hypothyroid status induced remodeling on putative synaptic contacts between NEI and dopaminergic neurons.

Effects of hypo- and hyperthyroidism in the DL-PLH

In the same trend of the previous results, the area located dorsal to the peduncular part of the lateral hypothalamus and lateral to the subincertal nucleus (DL-PLH, Fig. 1B, C, I-K) also showed dense networks of somas, fibers and terminals with NEI-IR. We were also able to observe a prevalence of TH-IR fibers running diagonally to the brain sagittal axis (Fig. 1K and Fig. 2G) and lack of presence of TH-IR somas. In this area, as before, we did not observe co-localization of both labels (Fig. 2G third row). The percentage of total NEI-IR (expressed as OD units, see methods) was not affected by the thyroid status (Fig. 2H) but the TH-IR decreased significantly in the hypoT animals ($p<0.01$ vs control) (Fig. 2I). When the NEI positive objects/NEI neuron were analyzed in the DL-PLH, a similar pattern was observed as in the IHy. The hypoT animals showed an increased and hyperT animals a decreased number of NEI positive objects/NEI positive cell ($p<0.05$ vs control) and also the treated groups showed differences among them ($p<0.001$) (Fig. 3C). When the TH-IR objects were counted, highly significant decreases were observed in the hypoT ($p<0.001$ vs control) and in the hyperT rats ($p<0.01$ vs control) (Fig. 4C). This last observation indicates that the DL-PLH area may be considerably responsive to changes in the thyroid status. Surprisingly, in the 3D analysis, the total number of NEI-TH contacts was not affected by the thyroid status (Fig.5M).

Effects of hypo- and hyperthyroidism in the PLH

We also decided to observe the characteristics of NEI and TH label in the PLH at -2.76 mm from Bregma. As it was expected, the view was similar to the one described before showing dense networks of NEI-IR somas, fibers and terminals and also numerous TH-IR fibers in close apposition (Fig. 6A-C).

To go deeper in the relationship between NEI neurons and the HPT axis, we decided to observe the relationship between NEI-IR and the distribution of thyrotrophic releasing hormone receptor-1 (TRH-R1), which is the main receptor responsible of the neuroendocrine action of TRH in the brain. For this, we used a total of 9 animals divided in three groups, control (n=3), hypoT (n=3) and hyperT (n=3). A profuse TRH-R1 labeling was observed throughout all taken images at -2.76 mm from Bregma, in the form of a dense mesh of puncta and labeled somas (Fig. 6E, H). The NEI-IR neurons display a very

intense TRH-R1 labeling (Fig. 6F, I) which is also present in other non-identified cells of this region. This last observation is described for the first time in the literature indicating a possible regulatory action of TRH over the NEI neurons present in this area. Regarding TRH-R1 mRNA expression no changes were observed in either hypoT or hyperT groups. As the PLH is a fairly large region ranging from -1.20 mm to -4.56 mm from Bregma, we decided to determine the effects of hypo- and hyperthyroidism on NEI precursor (ppMCH) and TH by the detection of its respective mRNA expression in the three hormonal conditions: hypoT, hyperT, and euthyroid or control animals. PLH was obtained by microdissection of 1 mm thickness coronal brain slices obtained at -2,16 and 2,76 from Bregma in an aluminum cold plate at 4 ºC [17] and processed for total RNA extraction. The mRNA NEI precursor showed a significant increase ($p<0.01$) in gene expression in the hypoT rats (Fig. 7A) while the mRNA expression of TH was not affected by hypoT or hyperT treatment (Fig. 7B and C). Regarding TRH-R1 mRNA expression no changes were observed in either hypoT or hyperT groups.

Discussion

In this work we corroborate that in restricted places of the hypothalamus of the rat, the cellular expression of Neuropeptide EI, and of TH, the regulatory enzyme of the synthesis of catecholamines, are modified by the levels of circulating thyroid hormones. On the other hand, we found that hypo- and hyperthyroidism induced modifications of the dendritic arbor of NEI expressing cells and in the number of TH expressing fibers and boutons. We also observed that NEI and dopaminergic neurons and fibers were closely related, establishing putative synaptic contacts that were increased by hypothyroidism in both the rostral and caudal-IHy region, while the DL-PLH was not affected. We also found co-localization and close contacts between NEI and thyrotrophic releasing hormone receptor-1 (TRH-R1) expressing neurons. However, a further analysis should be performed using electron microscopy or synaptophysin labeling to determine whether or not the close contacts identified in the present study by fluorescence microscopy represent true synaptic contacts.

It has been proposed that the dopaminergic neurons present in the IHy exert a regulatory activity on neuroendocrine functions that are mediated by the medial hypothalamus [26, 28]. On the other hand, most of the neurons containing MCH/NEI are located also within the incerto-hypothalamic and lateral hypothalamic areas [29]. Altogether, both groups of neurons seem to be regulated by thyroid hormones. Although T_3 is known to have significant effects on brain development, little is known about its role in the adult brain, particularly within the hypothalamic nuclei where many of the homeostatic control

neurons regulating reproduction, food intake, energy expenditure, glucose homeostasis, and thermoregulation are located.

The present results contribute to the previous observations about the changes at cellular and molecular level of NEI as a consequence of the complex modulatory activity of the HPT axis [16]. One interesting observation is that both experimental conditions, hypoT and hyperT, also induce responses of the peptidergic neurons and fibers containing NEI in hypothalamic areas additional to those described before. In a previous paper we informed that the NEI concentration measured in the perifornical part of the lateral hypothalamus (PeFLH), organum vasculosum of the lamina terminalis (OVLT) and anteroventral periventricular nucleus (AVPV) in the euthyroid female rat follows a cyclic pattern, and this characteristic is altered under the hypoT or hyperT status [17], suggesting that NEI is regulated by pituitary and ovarian hormones [17].

It was already known that hypothyroidism induced by propylthiouracil (PTU) decreases and hyperthyroidism induced by T_4 administration increases TH activity in the anterior part of the locus coeruleus and adrenal medulla [26]. Circulating levels of T_4 and T_3 control brain TH activity by altering the kinetic properties of the enzyme, which, in turn, influence catecholaminergic activity and consequently the modulatory effect on TRH and TSH [31, 32]. In previous work by Real Time–PCR our laboratory reported that at the end of pregnancy, TH mRNA expression increased in the medial basal hypothalamus after T_4 administration. In consequence, the hypothalamic negative short loop feedback, which regulates the PRL axis is disturbed in the hyperT rats, compromising lactation and pup survival [26]. In addition the TH positive neurons seem to co-express thyroid hormone receptors, meaning that the thyroid hormones act through their own receptors present in the hypothalamic dopaminergic neurons [33].

In the present study we further explored the action of the thyroid hormones on nerve terminals and fibers of the NEI and catecholaminergic systems in hypothalamic areas where an interaction may occur, particularly the IHy and DL-PLH. The rostromedial zona incerta (IHy) is thought to exert autonomous roles by integrating sensory input to autonomic, neuroendocrine, and motor output. It has been characterized as an area comprised between the medial hypothalamus and the ZI, along the brain rostro-caudal axis and chemically defined as comprising belonging to the A13 group and the neurons expressing MCH/NEI neurons [2, 4]. Using confocal microscopy with 3D reconstructions, we assessed changes in rostral- and caudal-IHy, and DL-PLH with two complementary approaches: measurements of overall NEI and TH immunoreactive density in these hypothalamic regions and quantification of

immunoreactive boutons and fibers overlapping NEI neurons and dendrites. On the other hand, we explored how dysthyroidism could cause morphological consequences in our experimental model of adult male rats. This approach is not novel, i.e. the effects of thyroid hormones on the size and the neurite length and arborization of hypothalamic dopaminergic neurons were studied previously in fetal brain cell cultures [34]. In the developing caudate nucleus, neonatal thyroid hormone deficiency reduces the number of neurons, the dendritic arborization, the number of dendritic spines and the complexity of the axonal plexus. In contrast, the size of neuron somata is not affected [35]. However, different brain regions may not respond equally [34, 35], Furthermore, the responses also depend on the degree of dysthyroidism as well on the brain area, the age and sex of the animals [16, 17, 26, 38]. In the caudal portion of the IHy we observed a decrease of TH immunostaining in the hypothyroid animals, indicating a regulation of these fibers by thyroid hormones, probably favoring dopaminergic activity in the euthyroid animal and restraining it in the animal with a disturbed thyroid axis. The relationship of NEI and the dopaminergic system in this area has not been previously explored. Most of the dopaminergic pathways seem to run closely to the MCH-NEI systems, but co-expression in the same neurons was not observed [3, 4]. A remodeling of the contacts between the dopaminergic and NEI terminals and somas is shown in this work, under prolonged exposure to thyroid hormone deficit.

We also included the analysis of the DL-PLH, an area defined by the following anatomical limits: the ventral part of the zona incerta (dorsal), the internal capsule (external), the subincertal nucleus (internal) and the peduncular part of the lateral hypothalamus (ventral). This area also contains NEI immunoreactive somas, which do not seem to be altered by the thyroid status. However, the arborization of these neurons seemed to be more conspicuous in the hypoT and decreased in the hyperT in relation to the euthyroid animal. Also in this area, we observed that the dopaminergic fibers are reduced in the treated animals, indicating a possible remodeling of the terminals although the interaction between DA and NEI elements seems to remain intact. This last observation suggests that at least in this area, the pattern of functional interaction among the cells is maintained despite the modifications in the number of NEI or TH objects induced by the thyroid hormonal status, although the exact mechanism of action of these hormones has not been established. Circulating T_4 is transported across the blood-brain barrier and enters astrocytes via specific transporters such as OATP1c1, where it is de-iodinated by type 2-deiodinase to produce T_3 [37]. T_3 is an important signaling factor that affects macro and microglial functions via complex mechanisms [37, 38] and it is widely known that glial cells play an important role in the neuroendocrine regulation of many physiological activities by

participating in the maturation and remodeling of neuronal connectivity of the different hypothalamic areas [39, 40]. Therefore, the observed changes in the distribution of terminals and boutons in the proximity of the somas of the neurons containing NEI could be explained by changes of glial architecture induced by the increase or decrease of thyroid hormones. T_3 and T_4 were shown to modulate the interactions between astrocytes and neurons, modifying the level and distribution of the extracellular matrix and cytoskeleton proteins and other components of the synaptic microenvironment that regulate neurite outgrowth [37]. Further work is needed to understand the effects of thyroid hormones on glia activity in the hypothalamic areas mentioned in this study.

In a previous work we observed that in known areas containing NEI terminals, the peptide content was modified by hypo- or hyperthyroidism. On the other hand, no differences among treatments were observed at PLH [16]. As NEI is synthetized as part of a pro-hormone (pp-MCH), we decided to observe if thyroid states could affect peptide synthesis in MCH/NEI neurons at PLH. Also the study on the PLH, an area populated with neurons that synthetize NEI in their somas, reinforced the concept that this peptide could be included in the circuit of the HPT axis exerting a regulatory action on the activity of the underlying neural paths. The increase in the levels of expression of NEI precursor (ppMCH) mRNA by the changes by hypothyroidism indicates that these neurons may be responsive to the action of TRH, and this concept is supported by the presence of TRH-R1 receptors on these neurons. On the contrary, the TH-mRNA content was not modified by the increase or decrease of the circulating thyroid hormones, in agreement with previous observations done by other authors. Altogether, these results suggest an additional level of ductility of the hypothalamic tissue where the cytoarchitecture and neurochemical connectivity can be modified under the influence of thyroid hormones.

In conclusion: we were able to observe effects of thyroid hormones over the NEI-IR neurons. These effects were hypothalamic region and circulating thyroid hormone levels dependent. By means of 3D reconstruction analysis we have shown that mainly hypothyroidism affected the number of contacts between NEI and TH somas, fibers and boutons in the IHy region, inducing a sensible remodeling of the putative synaptic contacts. However, this effect is not observed in the DL-PLH. On the other hand, under long-term hyperthyroid status, although the number of NEI and TH positive objects surrounding the neurons was changed, these systems seem to maintain a relative homeostatic pattern resembling the euthyroid condition. Finally, it was observed that MCH/NEI neurons at PLH express TRH-R1 receptor demonstrating the relationship between the HPT axis and MCH/NEI system.

Acknowledgements

This work has been supported by grant from PICT-R 32529 from Fondo para la Investigación Científica y Tecnológica (FONCyT), Agencia Nacional de Promoción Científica y Tecnológica (ANPCyT), Argentina and Programa I+D, Secretaría Ciencia, Técnica y Posgrado, Universidad Nacional de Cuyo, Cod. 06/P28 Res- 571/2015.

M.S., M.E.C., G.A.J., S.R.V. and AMS are Career Scientists from CONICET; C.A. and G.E.P. former CONICET fellows.

References

[1] Nahon JL, Presse F, Bittencourt JC, Sawchenko PE, Vale W: The rat melanin-concentrating hormone messenger ribonucleic acid encodes multiple putative neuropeptides coexpressed in the dorsolateral hypothalamus. Endocrinology 1989;125(4):2056-2065.

[2] Bittencourt JC, Presse F, Arias C, Peto C, Vaughan J, Nahon JL, Vale W, Sawchenko PE: The melanin-concentrating hormone system of the rat brain: an immuno- and hybridization histochemical characterization. 1992. J Comp Neurol 319(2):218-245.

[3] Elias CF, Sita LV, Zambon BK, Oliveira ER, Vasconcelos L a P, Bittencourt JC: Melanin-concentrating hormone projections to areas involved in somatomotor responses. J Chem Neuroanat 2008;35(2):188–201.

[4] Sita LV, Elias CF, Bittencourt JC: Dopamine and melanin-concentrating hormone neurons are distinct populations in the rat rostromedial zona incerta. Brain Res 2003;970(1-2):232-237.

[5] Attademo A, Sánchez-Borzone M, Lasaga M, Celis M: Intracerebroventricular injection of neuropeptide EI increases serum LH in male and female rats. Peptides 2004;25:1995–1999.

[6] Attademo AM, Rondini TA, Rodrigues BC, Bittencourt JC, Celis ME, Elias CF: Neuropeptide glutamic acid-isoleucine may induce luteinizing hormone secretion via multiple pathways. Neuroendocrinology 2006;83:313–324.

[7] Bittencourt JC, Celis ME: Anatomy, function and regulation of neuropeptide EI (NEI). Peptides 2008;29(8):1441-1450.

[8] Sánchez M, Baker BI, Celis M: Melanin-concentrating hormone (MCH) antagonizes the effects of α-MSH and neuropeptide E-I on grooming and locomotor activities in the rat. Peptides 1997; 18(3):393–396.

[9] Sánchez M, Barontini M, Armando I, Celis M: Correlation of increased grooming behavior and motor activity with alterations in nigrostriatal and mesolimbic catecholamines after α-melanotropin and neuropeptide glutamine-isoleucine injection in the rat ventral tegmental area. Cell Mol Neurobiol 2001;21(5):523–533.

[10] Berberian V, Sanchez M, Celis M: Participation of the cholinergic system in the excessive grooming behavior induced by neuropeptide (N) glutamic acid (E) isoleucine (I) amide (NEI). Neurochem Res 2002; 27(12): 1713–1717.

[11] Sánchez-Borzone ME, Attademo A, Baiardi G, Celis ME: Effect of beta-adrenoceptors on the behaviour induced by the neuropeptide glutamic acid isoleucine amide. Eur J Pharmacol 2007;568: 186–191.

[12] Gonzalez MI, Baker BI, Hole DR, Wilson CA: Behavioral effects of neuropeptide E-I (NEI) in the female rat: interactions with alpha-MSH, MCH and dopamine. Peptides 1998; 19(6):1007-16.

[13] Kizer JS, Palkovits M, Zivin J, Brownstein M, Saavedra JM, Kopin IJ: The effect of endocrinological manipulations on tyrosine hydroxylase and dopamine-beta-hydroxylase activities in individual hypothalamic nuclei of the adult male rat. Endocrinology 1974;95(3):799-812.

[14] Calzà L, Forrest D, Vennström B, Hökfelt T: Expression of peptides and other neurochemical markers in hypothalamus and olfactory bulb of mice devoid of all known thyroid hormone receptors. Neuroscience 2000;101(4):1001-1012.

[15] Sun Y, Lu X, Gershengorn MC: Thyrotropin-releasing hormone receptors similarities and differences. J Mol Endocrinol 2003;30(2):87-97.

[16] Ayala C, Valdez SR, Morero ML, Soaje M, Carreño NB, Sanchez MS, Bittencourt JC, Jahn GA, Celis ME: Hypo- and hyperthyroidism affect NEI concentration in discrete brain areas of adult male rats. Peptides 2011; 32(6): 1249-1254.

[17] Ayala C, Pennacchio GE, Soaje M, Carreño NB, Bittencourt JC, Jahn GA, Celis ME, Valdez SR: Effects of thyroid status on NEI concentration in specific brain areas related to reproduction during the estrous cycle. Peptides 2013; 49:74-80.

[18] Paxinos G, Atlas WC. The rat brain in stereotaxic coordinates. 7th ed. London: Elsevier Inc; 2007.

[19] Swanson, LW. Brain maps: Structure of the rat brain third edition, (2004).

[20] Swanson LW, Sanchez-Watts G, Watts AG. Comparison of melanin-concentrating hormone and hypocretin/orexin peptide expression patterns in a current parceling scheme of the lateral hypothalamic zone, Neurosci. Lett. 468 (2005) 12–17. doi:10.1016/j.neulet.2009.10.047.

[21] Sita LV, Elias CF, Bittencourt JC. Connectivity pattern suggests that incerto-hypothalamic area belongs to the medial hypothalamic system. Neuroscience. 148 (2007) 949–69. doi:10.1016/j.neuroscience.2007.07.010.

[22] Bittencourt JC. Anatomical organization of the melanin-concentrating hormone peptide family in the mammalian brain., Gen. Comp. Endocrinol. 172 (2011) 185–97. doi:10.1016/j.ygcen.2011.03.028.

[23] Semenenko FM, Cuello AC, Goldstein M, Lee KY, Sidebottom E: A monoclonal antibody against tyrosine hydroxylase: application in light and electron microscopy. J Histochem Cytochem 1986;34(6):817-821.

[24] Mueller NK, Di S, Paden CM, Herman JP: Activity-dependent modulation of neurotransmitter innervation to vasopressin neurons of the supraoptic nucleus. Endocrinology 2005; 146: 348–354.

[25] Higa-Taniguchi KT, Silva FC, Silva HM, Michelini LC, Stern JE: Exercise training-induced remodeling of paraventricular nucleus (nor)adrenergic innervation in normotensive and hypertensive rats. Am J Physiol Regul Integr Comp Physiol 2007; 292(4):R1717-1727.

[26] Pennacchio GE, Neira FJ, Soaje M, Jahn GA, Valdez SR: Effect of hyperthyroidism on circulating prolactin and hypothalamic expression of tyrosine hydroxylase, prolactin signaling cascade members and estrogen and progesterone receptors during late pregnancy and lactation in the rat. Mol Cell Endocrinol 2017; 442:40-50.

[27] Livak KJ, Schmittgen TD: Analysis of relative gene expression data using real-time quantitative PCR and the 2(-Delta Delta C (T)) Method. Methods 2001;25(4):402-408.

[28] Sita LV, Elias CF, Bittencourt JC: Connectivity pattern suggests that incerto-hypothalamic area belongs to the medial hypothalamic system. Neuroscience 2007;148(4):949-69.

[29] Bittencourt JC: Anatomical organization of the melanin-concentrating hormone peptide family in the mammalian brain. Gen Comp Endocrinol 2011;172(2):185-197.

[30] Claustre J, Balende C, Pujol JF: Influence of the thyroid hormone status on tyrosine hydroxylase in central and peripheral catecholaminergic structures. Neurochem Int 1996;28(3): 277–281.

[31] Chaube R, Joy KP: Thyroid hormone modulation of brain in vivo tyrosine hydroxylase activity and kinetics in the female catfish Heteropneustes fossilis. J Endocrinol 2003; 179(2):205-215.

[32] Zimmermann RC, Krahn LE, Klee GG, Ditkoff EC, Ory SJ, Sauer MV: Prolonged inhibition of presynaptic catecholamine synthesis with alpha-methyl-para-tyrosine attenuates the circadian rhythm of human TSH secretion. J Soc Gynecol Investig 2001; 8(3):174-8.

[33] Pennacchio GE, Acosta CG, Seltzer AM, Soaje M, Jahn GA, Valdez, SR: Hyperthyroidism modulates hypothalamic tyrosine hydroxylase activity and PRL signaling during late pregnancy and early lactation in rats. 46th Annual Meeting of Society of Neuroscience. 2016. San Diego .CA Online program #/Poster#:813.08/PP10

[34] Puymirat J: Effects of dysthyroidism on central catecholaminergic neurons. Neurochem Int 1985; 7(6):969-977.

[35] Lu EJ, Brown WJ, Cole R, deVellis J: Ultrastructural differentiation and synaptogenesis in aggregating rotation cultures of rat cerebral cells. J Neurosci Res 1980; 5(5):447-463.

[36] Schroeder AC, Privalsky ML. Thyroid hormones, t3 and t4, in the brain. Front Endocrinol (Lausanne) 2014; 5:40.

[37] Dezonne RS, Lima FR, Trentin AG, Gomes FC: Thyroid hormone and astroglia: endocrine control of the neural environment. J Neuroendocrinol 2015; 27(6):435-445.

[38] Luo M, Puymirat J, Dussault JH: Immunocytochemical localization of nuclear 3,5,3'-triiodothyronine (L-T3) receptors in astrocyte cultures. Brain Res Dev Brain Res. 1989;46(1):131-136.

[39] Garcia-Segura LM, Lorenz B, DonCarlos LL: The role of glia in the hypothalamus: implications for gonadal steroid feedback and reproductive neuroendocrine output. Reproduction 2008; 135(4):419–429.

[40] Nuzzaci D, Laderrière A, Lemoine A, Nédélec E, Pénicaud L, Rigault C, Benani A: Plasticity of the Melanocortin System: Determinants and Possible Consequences on Food Intake. Front Endocrinol (Lausanne) 2015; 6:143.

Legends to the Figures:

Fig. 1. Anatomical background and representation of the acquired images and areas studied at -2.76 mm of distance from Bregma in a control animal (euthyroid). **A**: The framed area represents the region visualized at 20x magnification with the anatomical parameters, adapted from The Atlas: The Rat Brain in Stereotaxic Coordinates, Paxinos G & Watson Ch., 2007. **B**. Immunofluorescence image acquired in a confocal microscope at 20x magnification showing NEI positively stained neurons (green: labeled with FITC) and TH fibers (red: labeled with Cy5), distribution of NEI-IR cells is signed according to the different regions localized at this section, scale bar: 300 µm. **C**: Immunohistochemistry stained with DAB showing NEI distribution at -2.76 mm from Bregma, see that the distribution is the same observed in B. **D** and **E** show single channel images of NEI and TH (green and red respectively) of image B. **F**, **G** and **H**: Representative images acquired at xyz plane with 60x oil lents at the caudal-IHy of a control (euthyroid animal) which was first localized with the 20x objective (see framed area in B). **F** and **G**: Show single channels of NEI (green: labeled with FITC) and TH (red: labeled with Cy5) respectively at the caudal-IHy; **H**: Merge of both channels demonstrating the proximity of NEI cells and boutons with TH terminals in this region. **I**, **J** and **K**: Representative images acquired at xyz plane with 60x oil lents at the DL-PLH of a control (euthyroid animal) which was first localized with the 20x objective (see framed area in B). **I** and **J**: Show single channels of NEI (green: labeled with FITC) and TH (red: labeled with Cy5) respectively at the DL-PLH; **K**: Merge of both channels demonstrating the proximity of NEI cells and boutons with TH terminals in this region. Abbreviations of the structures shown in this figure are: caudal-IHy: caudal portion of the incerto-hypothalamic area, DL-PLH: dorsolateral zone of the peduncular part of the lateral hypothalamus, PLH: peduncular part of the lateral hypothalamus, f: fornix, PeF: perifornical nucleus, PeFLH: perifornical part of the lateral hypothalamus.

Fig. 2. Effect of hypo- (hypoT) and hyperthyroidism (hyperT) on Neuropeptide glutamic-acid-isoleucine amide (NEI) and Tyrosine Hydroxylase (TH) expression in the incerto-hypothalamic area (IHy) and in the dorsolater zone of the peduncular part of the hypothalamus (DL-PLH). A total of 9 animals were used for this analysis divided in control (n=3), hypoT (n=3) and hyperT (n=3) groups. The intensity of labeling and the effect of treatments, NEI and TH immunoreactivity (IR) were analyzed in terms of optical density (OD). Hypothyroidism caused the major changes on NEI and TH labeling

in these areas. Panels **A**, **D** and **G** show immunofluorescence of positively stained neurons for NEI (first line, at 8 bits) and TH neurons and fibers (second line, at 8 bits), green (NEI: labeled with FITC) and red (TH: labeled with Cy5) channels are merged in the third line. Images from rostral and caudal-IHy (rostral-IHy: at -2.16 mm from Bregma and caudal-IHy: at -2.76 mm from Bregma) and DL-PLH: at -2.76 mm from Bregma, belong to euthyroid (control), hypothyroid (hypoT) and hyperthyroid (hyperT) rats. Scale Bar: 20 μm. **B** and **C** (rostral-IHy), **E** and **F** (caudal-IHy), **H** and **I** (DL-PLH) represent quantification of NEI and TH optical density (OD) in each area studied. HypoT increased NEI OD in the IHy (B and E) and diminished TH OD in caudal-IHy and DL-PLH (F and I). Each column represents mean ± SEM, * p< 0.05, ** p< 0.01, *** p< 0.001 (number of NEI cells considered by treatment and region studied are indicated in Material and Methods: (number of NEI cells considered by treatment and region studied are indicated in Material and Methods: control:12, hypoT:21 and hyperT:8 in the rostral-IHy respectively; control: 26, hypoT: 27 and hyperT: 21 in the caudal-IHy and control: 27, hypoT: 25 and hyperT: 25 in the DL-PLH.).

Fig. 3. Effect of hypo (hypoT) and hyperthyroidism (hyperT) in the number of tridimensional (3D) objects (dendrites and boutons) of Neuropeptide glutamic-acid-isoleucine amide (NEI) in the incerto-hypothalamic area (IHy) and in the dorsolateral zone of the peduncular part of the lateral hypothalamus (DL-PLH). **A**, **B** and **C** show the relative quantification of NEI 3D-objects in each area and group under study (**A**: rostral-IHy, **B**: caudal-IHy and **C**: DL-PLH) of control (euthyroid, n=3), hypothyroid (hypoT, n=3) and hyperthyroid (hyperT, n=3) rats. Each column represents mean ± SEM, * $p< 0.05$, ** $p< 0.01$, *** $p< 0.001$, (number of NEI cells considered by treatment and region studied are indicated in Material and Methods as is indicated also in figure 2).

Fig. 4. Effect of hypo (hypoT) and hyperthyroidism (hyperT) in the number of tridimensional Tyrosine Hydroxylase immunoreactive objects (TH-IR-3D objects: dendrites and boutons) in the incerto-hypothalamic area (IHy) and in the dorsolateral zone of the peduncular part of the hypothalamus (DL-PLH). A, B and C show the relative quantification of TH-IR 3D-objects in each area and group under study (**A**: rostral-IHy, **B**: caudal-IHy and **C**: DL-PLH) of control (euthyroid, n=3), hypothyroid (hypoT, n=3) and hyperthyroid (hyperT, n=3) rats. Each column represents mean ± SEM, $p< 0.05$, ** $p< 0.01$, *** $p< 0.001$.

Fig. 5. Tridimensional (3D) reconstruction of Neuropeptide glutamic acid-isoleucine amide immunoreactive neurons dendrites, axons and end-boutons (NEI-IR) and Tyrosine Hydroxylase somas

and fibers (TH-IR) in the rostral-IHy. A representative assembly of a euthyroid animal as an example. Graphs represent the quantification of NEI and TH juxtapositions (contacts) of all groups studied. **A**: Immunofluorescence image of NEI (green: labeled with FICT) and TH (red:labeled with Cy5) in the IHy in XYZ; B and E are the enlargement of the framed area in A. **B**: NEI-IR soma, axon and varicosities; **E**: TH-IR somas, dendrites, axon and boutons. **C** and **D** show the 3D reconstruction of B; **F** and **G** show the 3D reconstruction of E; **H**: Merge of images B and E.; **I** and **J** show the 3D reconstruction of H. Scale bar: 20 μm. K, L and M show the results of the tridimensional analysis of NEI-TH contacts expressed as % of total NEI-TH contacts in each area and group under study (**K**: rostral-IHy, at -2.16 mm from Bregma; **L**: caudal-IHy; **M**: DL-PLH both at -2.76mm from Bregma) of control (euthyroid, n=3), hypothyroid (hypoT, n=3) and hyperthyroid (hyperT, n=3) rats. Hypothyroidism increased the number of NEI–TH contacts in rostral and dorsal IHy but not in the DL-PLH. Each column represents mean ± SEM, * $p< 0.05$, *** $p< 0.001$.

Fig. 6. NEI, TH and TRH-R1 immunofluorescence in the peduncular part of the lateral hypothalamus (PLH) of a control (euthyroid) animal at -2.76 mm from Bregma. **A** and **D**: NEI/ FITC labeled neurons and their dendritic arbors. **G**: magnification of the area limited by the rectangle in panel **D**. **B**: TH/Cy5 immunolabeled fibers. In this area the closeness of NEI-neuronal somas and TH-fibers is observed merged of both channels is shown in panel **C**. **E**: TRH-R1/Alexa 568 immunolabeled elements are shown. H: 60x magnification of the area included in the rectangle drawn in panel E. **F**: Merge image of green and red channels showing co-localization of the TRH-R1 immunolabeled elements on the NEI neurons. **I**: an enlarged view (60x) of the area included in the rectangle drawn in F. Scale bar: 20 μm. A total of 18 animals were used for these experiments, 9 to analyze the relationship between NEI and TH, divided in 3 per group studied and other 9 animals for the analysis of the colocalization of TRH-R1 in NEI expressing somas, divided also in the tree conditions: control (euthyroid, n=3), hypoT (n=3) and hyperT (n=3).

Fig. 7. Effect of hypo- (hypoT) and hyperthyroidism (hyperT) on the genomic expression of NEI precursor, TH and TRH-R1 in the peduncular portion of the lateral hypothalamus (PLH). **A**: relative NEI precursor mRNA expression normalized to S16; **B**: relative TH mRNA /S16 ratio; **C**: TRH-R1/ S16 ratio. Each column represents mean ± SEM, * $p< 0.05$, n= 10 animals per each group, ANOVA-1 followed by Bonferroni multiple comparisons post-test.

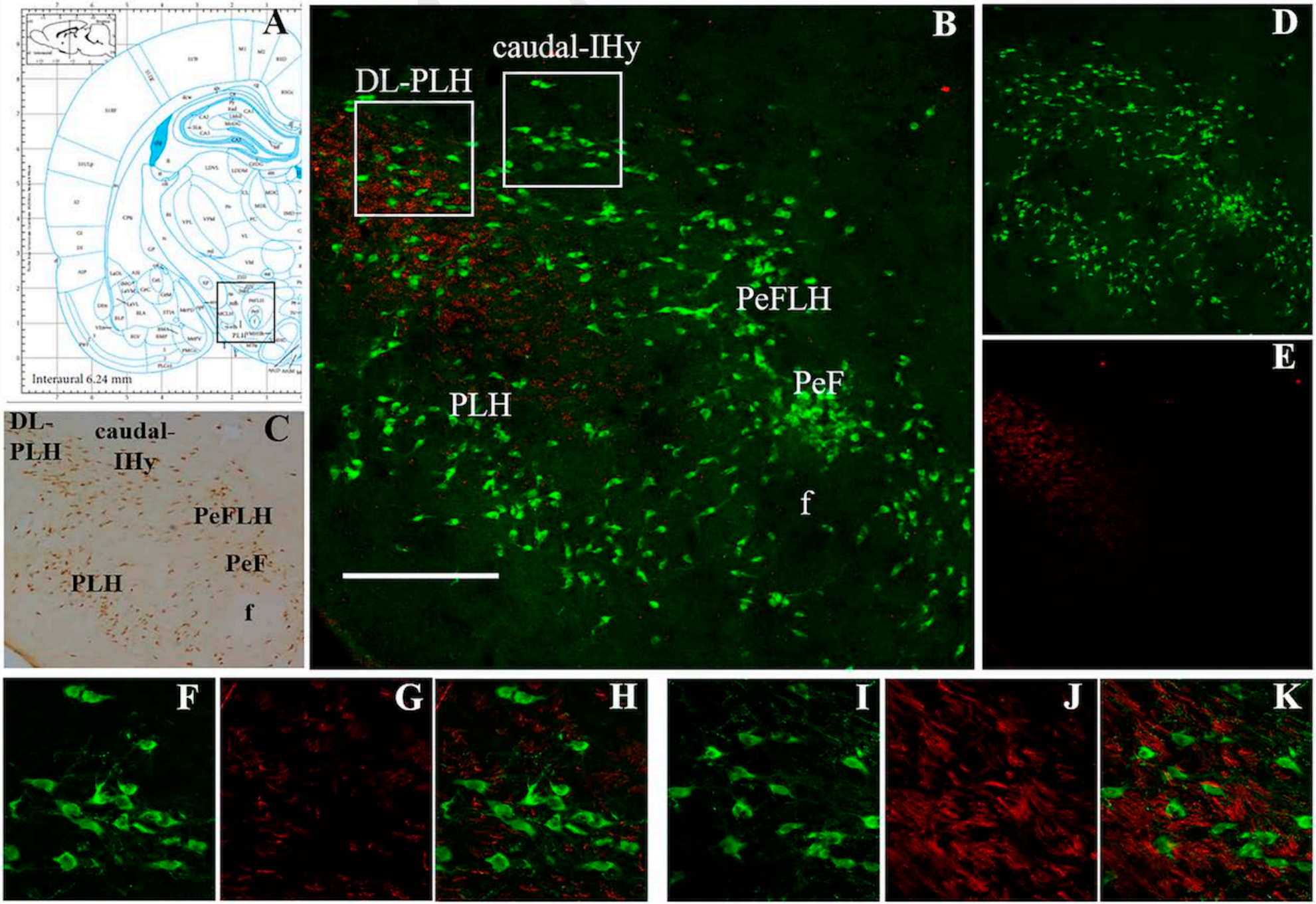
A
Interaural 6.24 mm
B
DL-PLH
caudal-IHy
PeFLH
PeF
PLH
f
C
DL-PLH
caudal-IHy
PeFLH
PeF
PLH
f
D
E
F
G
H
I
J
K

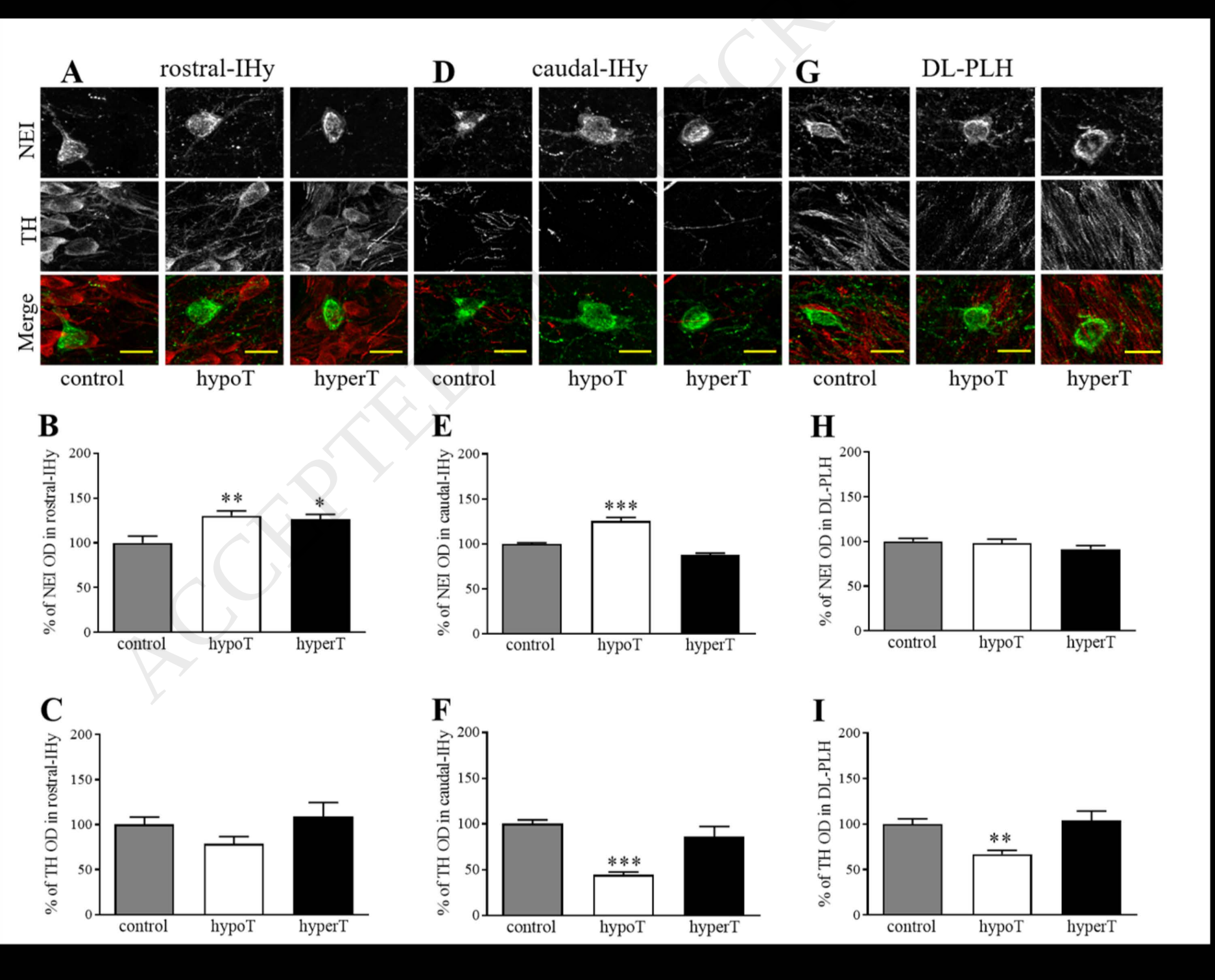
A
rostral-IHy
D
caudal-IHy
G
DL-PLH
NEI
TH
Merge
control
hypoT
hyperT
control
hypoT
hyperT
control
hypoT
hyperT
B
% of NEI OD in rostral-IHy
200
150
100
50
0
**
*
control
hypoT
hyperT
E
% of NEI OD in caudal-IHy
200
150
100
50
0
***
control
hypoT
hyperT
H
% of NEI OD in DL-PLH
200
150
100
50
0
control
hypoT
hyperT
C
% of TH OD in rostral-IHy
200
150
100
50
0
control
hypoT
hyperT
F
% of TH OD in caudal-IHy
200
150
100
50
0
***
control
hypoT
hyperT
I
% of TH OD in DL-PLH
200
150
100
50
0
**
control
hypoT
hyperT

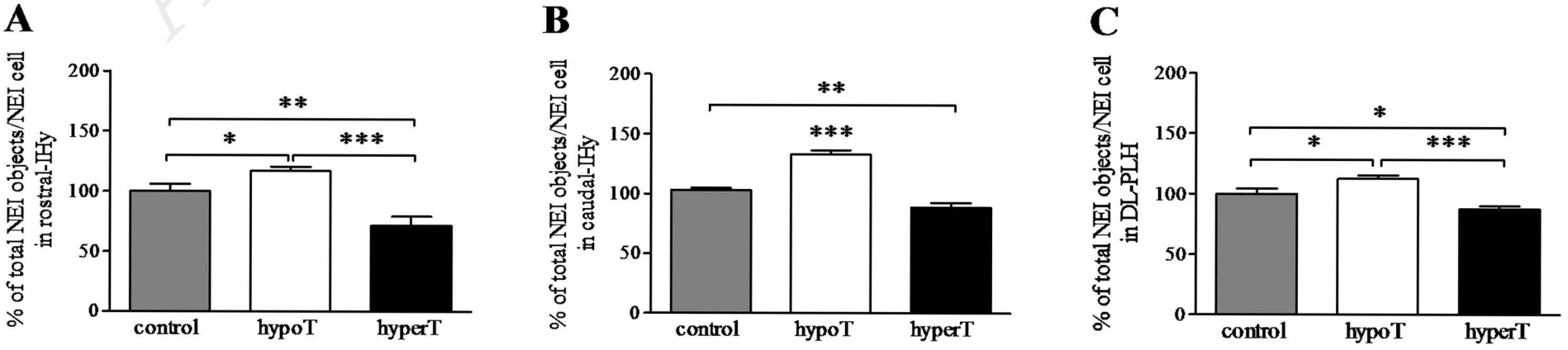
A
% of total NEI objects/NEI cell in rostral-IHy
200
150
100
50
0
**
*
***
control
hypoT
hyperT
B
% of total NEI objects/NEI cell in caudal-IHy
200
150
100
50
0
**
***
control
hypoT
hyperT
C
% of total NEI objects/NEI cell in DL-PLH
200
150
100
50
0
*
*
***
control
hypoT
hyperT

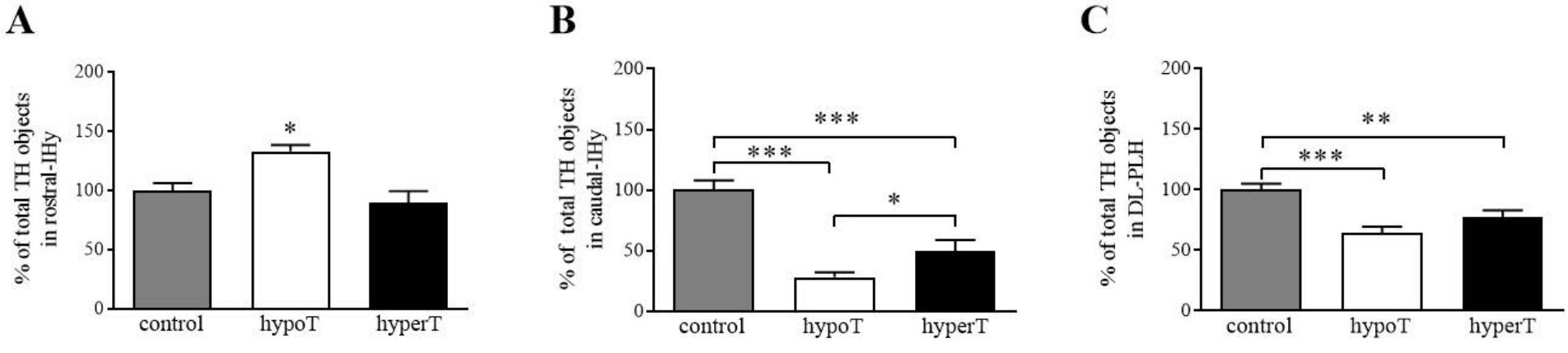
A
% of total TH objects in rostral-IHy
200
150
100
50
0
*
control
hypoT
hyperT
B
% of total TH objects in caudal-IHy
200
150
100
50
0
***
***
*
control
hypoT
hyperT
C
% of total TH objects in DL-PLH
200
150
100
50
0
**
***
control
hypoT
hyperT

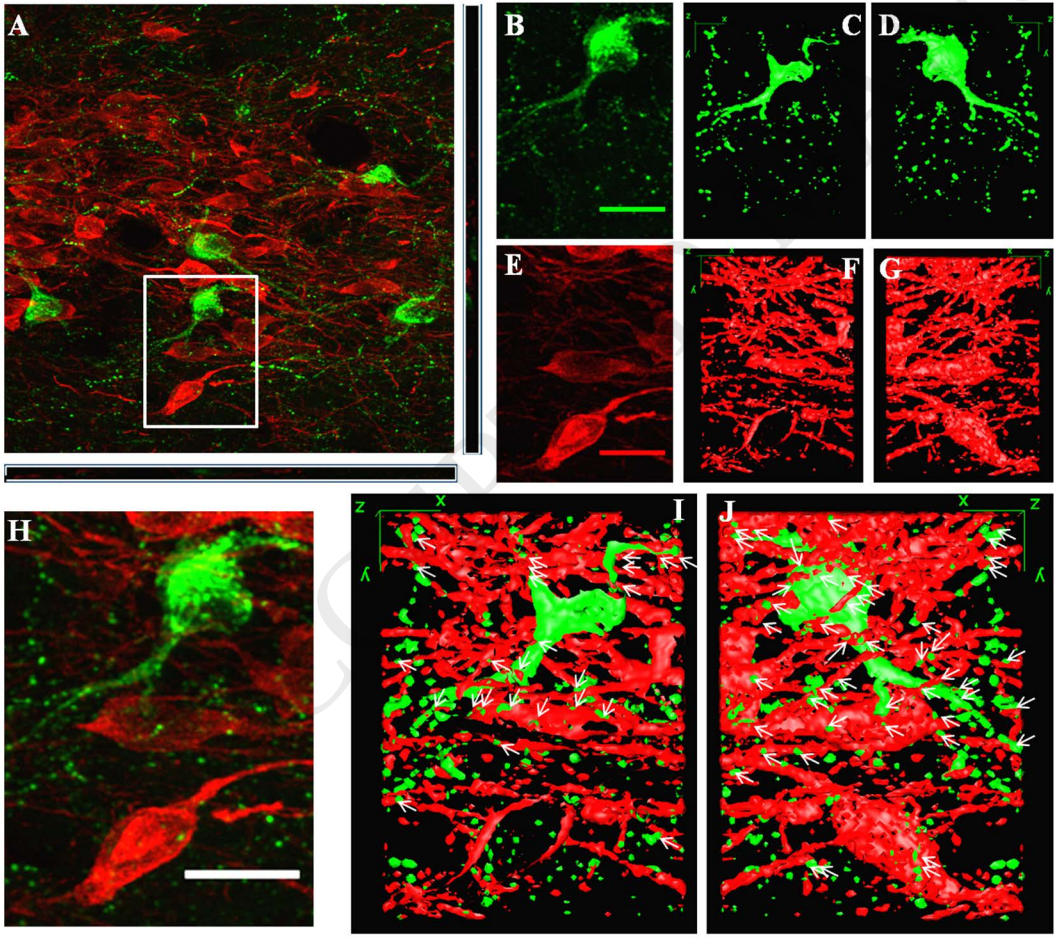
A
B
C
D
E
F
G
H
I
J
K
% of total NEI-TH contacts in rostral-HIy
400
300
200
100
0
*
control
hypoT
hyperT
L
% of total NEI-TH contacts in caudal-HIy
***
M
% of total NEI-TH contacts in DL-PLH

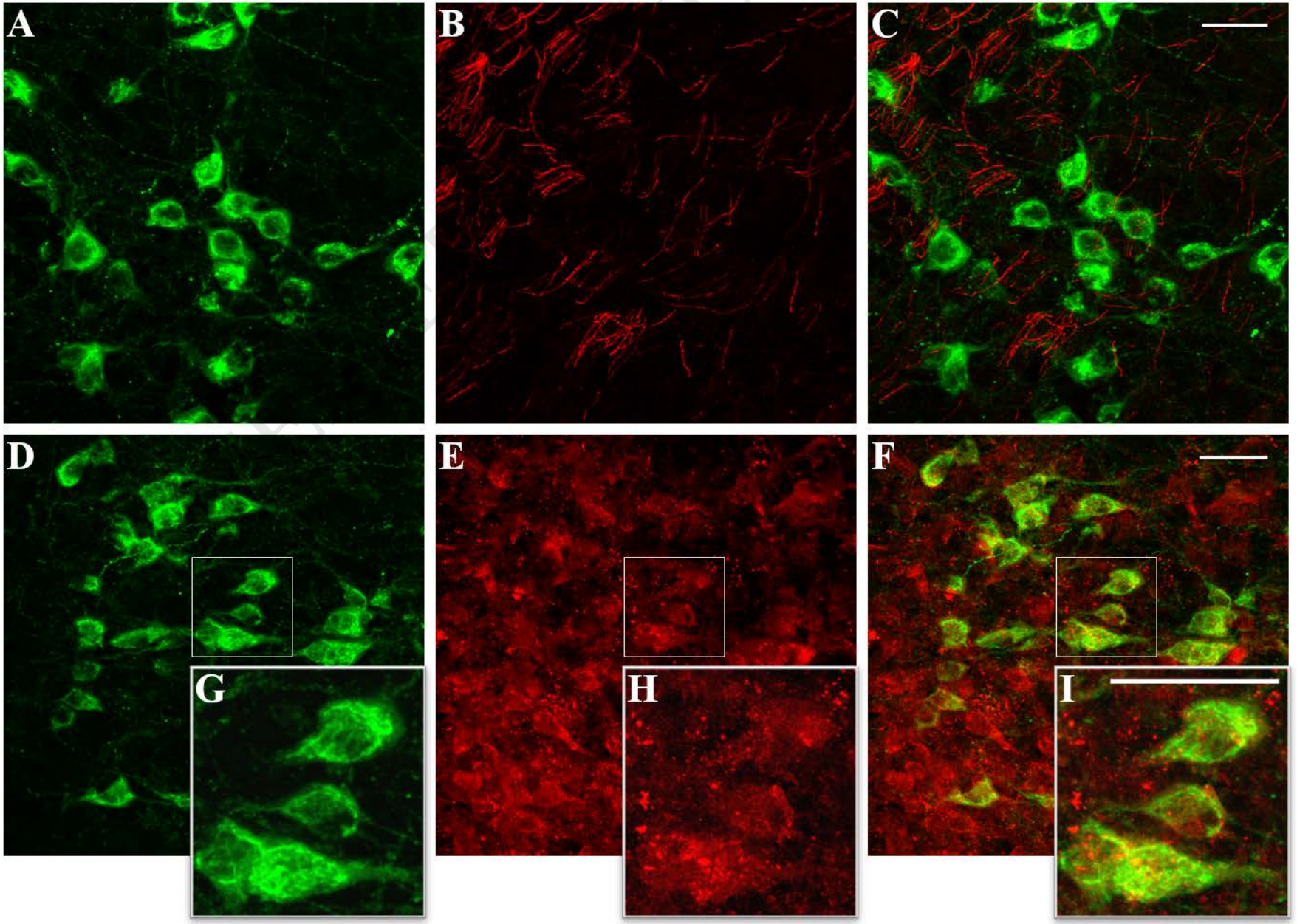
A
B
C
D
E
F
G
H
I

A

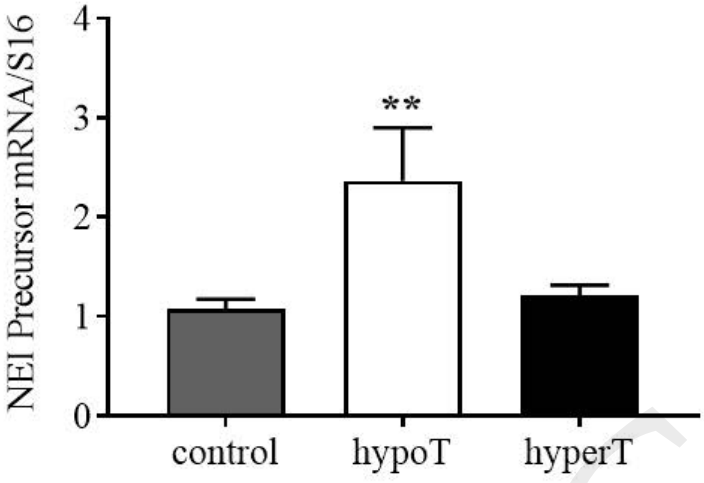
NEI Precursor mRNA/S16
4
3
2
1
0
**
control
hypoT
hyperT

B

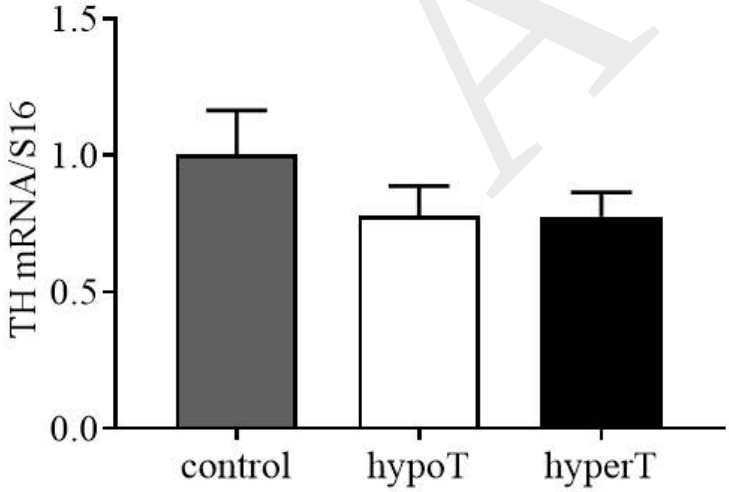
TH mRNA/S16
1.5
1.0
0.5
0.0
control
hypoT
hyperT

C

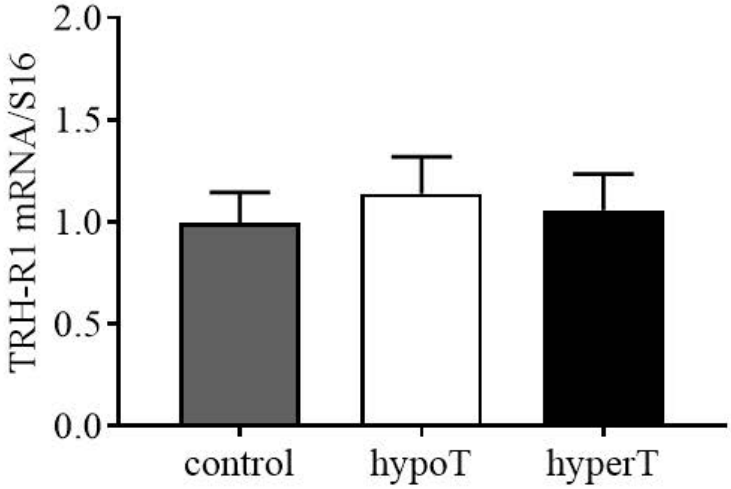
TRH-R1 mRNA/S16
2.0
1.5
1.0
0.5
0.0
control
hypoT
hyperT